コヒーレントノイズ下の表面符号における
フォールトトレラント量子誤り訂正の
サンプリングに基づいたシミュレーション

八角 繁男[1,a)]　御手洗 光祐[1,3,2,b)]　藤井 啓祐[1,3,4,c)]

概要：本研究では、コヒーレントノイズ下でのフォールトトレラント量子誤り訂正のサンプリングに基づいたシミュレーション方法を提案する。このシミュレーションでは、過回転に起因するコヒーレントノイズとインコヒーレントノイズの混合ノイズを擬確率分布により Clifford チャンネルに分解する。そして、適切な後処理を施し Clifford チャンネルをサンプルすることで、論理エラー率の不偏推定量を構成する。また、チャンネルロバストネスによりサンプリングコストを評価することを通じて、フルベクトルシミュレーションでは困難な比較的大きな符号距離を持つ平面表面符号ですら、提案したサンプリングベースの手法が実行可能であることを示した。デモンストレーションとして、符号距離が 5 で 81 量子ビットからなる平面表面符号のノイズのある反復的なシンドローム測定をシミュレーションした。その結果、コヒーレントエラーにより論理エラーが増加することを示した。これは、擬確率分布シミュレーションを意味のある課題に実用化したものであり、近未来の量子デバイス上で実験的に量子誤り訂正を研究する上で有用である。

Sampling-based quasi-probability simulation
for fault-tolerant quantum error correction
on the surface codes under coherent noise

Hakkaku Shigeo[1,a)]　Mitarai Kosuke[1,3,2,b)]　Fujii Keisuke[1,3,4,c)]

Abstract: We propose a sampling-based simulation for fault-tolerant quantum error correction under coherent noise. A mixture of incoherent and coherent noise, possibly due to over-rotation, is decomposed into Clifford channels with a quasiprobability distribution. Then an unbiased estimator of the logical error probability is constructed by sampling Clifford channels with appropriate post-processing. We characterize the sampling cost via the channel robustness and find that the proposed method is feasible even for planar surface codes with relatively large code distances intractable for full state-vector simulations. We simulate repetitive faulty syndrome measurements on the planar surface code of distance 5 with 81 qubits as a demonstration. We find that the coherent error increases the logical error rate. This is a practical application of the quasiprobability simulation for a meaningful task and would be useful to explore experimental quantum error correction on the near-term quantum devices.

1　大阪大学基礎工学研究科
　　Graduate School of Engineering Science, Osaka University, 1-3 Machikaneyama, Toyonaka, Osaka 560-8531, Japan
2　JST さきがけ
　　JST, PRESTO, 4-1-8 Honcho, Kawaguchi, Saitama 332-0012, Japan
3　量子情報・量子生命研究センター
　　Center for Quantum Information and Quantum Biology,

Osaka University, 1-2 Machikaneyama, Toyonaka 560-0043, Japan
4　理研 量子コンピュータ研究センター
　　RIKEN Center for Quantum Computing (RQC), Hirosawa 2-1, Wako, Saitama 351-0198, Japan
a)　shigeo.hakkaku@qc.ee.es.osaka-u.ac.jp
b)　mitarai@qc.ee.es.osaka-u.ac.jp
c)　fujii@qc.ee.es.osaka-u.ac.jp

---

1. Introduction

Quantum error correction (QEC) is an essential ingredient for developing scalable fault-tolerant quantum computers because quantum information is vulnerable to environmental noise [1], [2]. QEC counteracts noise by encoding quantum information into a subspace of multiple qubits, which assures computation with arbitrary precision in quantum computers. Massive experimental efforts have been devoted to demonstrating small-scale QEC circuits as testbeds toward large-scale QEC circuits in the future as well as numerical simulations [3], [4], [5]. It is thus important to investigate performances of QEC codes theoretically to establish a plausible goal for experiments.

Most numerical studies for QEC have been conducted by assuming stochastic Pauli noise to exploit the efficient simulatability of stabilizer states [6], [7]. Specifically, Ref. [8] numerically calculated the threshold error rate of the rotated surface code under single- and two-qubit depolarizing channels with circuit-level noise and observed a threshold error rate of 0.57%. This result suggests that the surface code can cope with the error rate that current state-of-the-art quantum computers are reaching [5], [9]. While the computational overhead increases when compared to the Pauli noise, we can also efficiently simulate the Clifford noise such as stochastic Clifford gates and Pauli projections.

In practice, however, quantum devices often suffer from noise that cannot be described by Clifford operations. A major type of such noise is coherent unitary noise which is caused by the miscalibration of quantum gates which leads to over- or under-rotations. Ref. [10] has developed a method to detect over-rotation errors using randomized benchmarking and detected $\pi/128$ over- or under-rotation errors in their superconducting qubit. While the error has been calibrated subsequently in Ref. [10], one can expect that a small amount of such errors beyond the experimental sensitivity are still present.

Analysis of the performance of QEC in such realistic situations still remains a challenge. QEC circuits under non-Clifford noise have been investigated either by brute-force simulations [11], [12] or by exploiting exact solvability of free fermion dynamics [13], [14]. However, full state-vector simulations require exponential computational resource with respect to the code distance and are currently limited to distance-3 surface code which uses 25 qubits [11]. While the use of approximate simulation using tensor network [12] has pushed the limit to 153 qubits

with perfect syndrome measurements, it is still difficult to scale up the simulation. On the other hand, free fermion simulations can handle coherent errors in a scalable manner. However, their usage is limited to certain cases: one-dimensional repetition codes with faulty syndrome measurements [13] which can only correct X errors and surface codes with perfect syndrome measurements [14].

In this work, we propose a sampling-based simulation method widely applicable for fault-tolerant QEC circuits under a mixture of coherent and incoherent noise with multiple rounds of faulty syndrome measurements. The central idea is to decompose (possibly non-Clifford) noise channels into the sum of completely stabilizer preserving (CSP) channels [15]. We simulate the circuits by sampling CSP channels according to quasi-probability distributions, which is obtained from the decompositions [15], [16]. Each realization is efficiently simulable since the simulation of CSP channels involves only stabilizer states. Note that Bennink *et al.* have conducted similar simulations for small systems such as Steane's 7-qubit code [16]. We significantly improve the computational cost required for the simulation by providing more efficient decomposition of noise channels than Ref. [16]. This reveals that we can perform an efficient simulation in the presence of coherent errors without any additional overhead for a wide range of practically interesting parameter region. Furthermore, even outside this region, the proposed quasi-probability method enables us to simulate a surface code of distance 5 with 81 qubits on a single workstation within a reasonable computational time.

As demonstrations, we simulate the planar surface code under the code capacity coherent noise with distance up to $d = 7$ and under the phenomenological coherent noise with distance up to $d = 5$. The result shows that such non-Clifford noise deteriorates the logical error rate as expected. We also evaluated how many samples are required to simulate the logical error rate reliably as a function of the noise parameters and the code distance. This reveals that the proposed method allows us to simulate the planar surface code with relatively large code distances, which are intractable for full state-vector simulations, with a reasonable computational overhead. The proposed method provides a benchmark for building small-scale fault-tolerant quantum computers in the NISQ era.

2. Simulation of QEC circuits under coherent noise

In this section, we discuss how to calculate a logical er-

ror rate of a QEC code by simulating quantum circuits with a quasi-probability sampling of CSP channels. QEC requires two types of qubits: data qubits, which constitute logical qubits, and measurement qubits, which are used for detecting errors on data qubits. The measurements extract eigenvalues of code stabilizers by measuring the latter, and these eigenvalues are called error syndromes. For a distance d code, we repeat such measurements for d rounds. We use a (noisy) Clifford circuit $\mathcal{E}_{\text{synd}}$ for the repetitive syndrome measurements. The measurement qubits of different rounds are to be treated as different qubits to simplify the notation. Let b be the error syndrome in space and time. When data qubits are initialized to $|0_L\rangle$, the probability of obtaining a specific error syndrome b is given by

$$p(b) = \langle b | \text{Tr}_{\text{data}} \left[\mathcal{E}_{\text{synd}} \left(|0_L\rangle\langle 0_L| \otimes |0^{|b|}\rangle\langle 0^{|b|}| \right) \right] |b\rangle \quad (1)$$

where $|b\rangle$ and $|0^{|b|}\rangle$ are final and initial states of the measurement qubits. After the extraction of error syndrome, we feed b to decoding algorithms such as a minimum-weight perfect-matching algorithm to find a possible recovery operation $\mathcal{R}_b$ which corrects errors on data qubits.

To express the logical error probability p_L in a closed form, we define the following infidelity function:

$$F(\rho) := 1 - \langle 0_L | \text{Tr}_{\text{meas}}[\rho] | 0_L \rangle. \quad (2)$$

Using Eqs. (1) and (2), p_L can be written as,

$$p_L = \sum_b F\left(\mathcal{R}_b \circ \mathcal{P}_b \circ \mathcal{E}_{\text{synd}} \left(|0_L\rangle\langle 0_L| \otimes |0^{|b|}\rangle\langle 0^{|b|}| \right) \right),$$

$$(3)$$

where $\mathcal{P}_b$ is the projection onto $|b\rangle\langle b|$. If the noise introduced in $\mathcal{E}_{\text{synd}}$ is a stochastic Pauli or Clifford error, one can simulate $\mathcal{E}_{\text{synd}}$ efficiently and can estimate the logical error rate p_L. However, efficient simulatability vanishes if noise involves non-Clifford channels.

We now describe an idea to deal with more general noise by a quasi-probability method [15], [16], [17], [18], [19], [20], [21], [22]. $\mathcal{E}_{\text{synd}}$ can be decomposed into (noisy) elementary operations as $\mathcal{E}_{\text{synd}} = \mathcal{E}^{(L)} \circ \cdots \circ \mathcal{E}^{(1)}$. Here L is the total number of quantum operations in $\mathcal{E}_{\text{synd}}$. $\mathcal{E}^{(i)}$ can be decomposed over CSP and completely positive trace-preserving (CPTP) channels $\mathcal{S}_k^{(i)}$ in terms of a quasi-probability distribution $c_k^{(i)}$ as,

$$\mathcal{E}^{(i)} = \sum_k c_k^{(i)} \mathcal{S}_k^{(i)}.$$

This decomposition can alternatively be written as,

$$\mathcal{E}^{(i)} = \sum_k p_k^{(i)} R_*\left(\mathcal{E}^{(i)}\right) \text{sign}\left(c_k^{(i)}\right) \mathcal{S}_k^{(i)},$$

where

$$R_*(\mathcal{E}) := \min_{\{c_k\}} \left\{ \sum_k |c_k|; \mathcal{E} = \sum_k c_k \mathcal{S}_k \right\},$$

$$p_k^{(i)} := \frac{\left| c_k^{(i)} \right|}{R_*\left(\mathcal{E}^{(i)}\right)}.$$

$R_*(\mathcal{E})$ is called channel robustness [15], the square of which characterizes the sampling cost, as will be seen later. Using this decomposition for each $\mathcal{E}^{(i)}$, $\mathcal{E}_{\text{synd}}$ becomes,

$$\mathcal{E}_{\text{synd}} = \sum_{\vec{k}} p_{\vec{k}} R_{*\text{tot}} \lambda_{\vec{k}} \mathcal{S}_{\vec{k}}, \quad (4)$$

where the summation is taken over all possible $\vec{k} = \left(k^{(1)}, k^{(2)}, \ldots, k^{(L)}\right)$, and

$$|\mathbf{0}\rangle\langle\mathbf{0}| := |0_L\rangle\langle 0_L| \otimes |0^{|b|}\rangle\langle 0^{|b|}|,$$

$$p_{\vec{k}} := \prod_{i=1}^{L} p_{k^{(i)}}^{(i)},$$

$$\lambda_{\vec{k}} := \prod_{i=1}^{L} \text{sign}\left(c_{k^{(i)}}^{(i)}\right),$$

$$\mathcal{S}_{\vec{k}} := \mathcal{S}_{k^{(L)}}^{(L)} \circ \cdots \circ \mathcal{S}_{k^{(1)}}^{(1)},$$

$$R_{*\text{tot}} := \prod_{i=1}^{L} R_*\left(\mathcal{E}^{(i)}\right).$$

Finally, combining Eqs. (3) and (4) we conclude,

$$p_L = \sum_b \sum_{\vec{k}} p_{\vec{k}} R_{*\text{tot}} \lambda_{\vec{k}} F\left(\mathcal{R}_b \circ \mathcal{P}_b \circ \mathcal{S}_{\vec{k}}(|\mathbf{0}\rangle\langle\mathbf{0}|) \right).$$

This implies that, when $\vec{k}$ is sampled from $p_{\vec{k}}$, $R_{*\text{tot}} \lambda_{\vec{k}} F\left(\mathcal{R}_b \circ \mathcal{P}_b \circ \mathcal{S}_{\vec{k}}(|\mathbf{0}\rangle\langle\mathbf{0}|) \right)$ is an unbiased estimator for p_L. Since it is bounded in a range $[-R_{*\text{tot}}, R_{*\text{tot}}]$, from Hoeffding inequality [23], the number of samples M needed to estimate p_L within additive error ϵ with probability at least $1 - \delta$ is given by

$$M = \frac{2}{\epsilon^2} R_{*\text{tot}}^2 \ln\left(\frac{2}{\delta}\right). \quad (5)$$

Note that, when we only consider Clifford noise, $\frac{2}{\epsilon^2} \ln\left(\frac{2}{\delta}\right)$ samples suffice to achieve the same accuracy. Therefore, $R_{*\text{tot}}^2$ quantifies the additional overhead required for including the effect of non-Clifford channels.

3. Planar surface codes under coherent noise

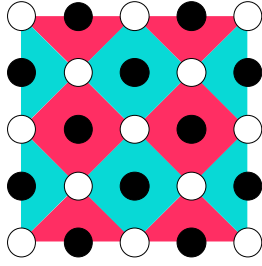To demonstrate the feasibility of the proposed method,

図 1 Layout of $d = 3$ planar surface code. The white and black circles represent data and measurement qubits, respectively. The light blue square and triangular patches show X stabilizers. The red square and triangular patches show Z stabilizers.

we consider the planar surface code introduced in Ref. [24], which is thought to be one of the most promising candidates for an experimental realization of QEC, as they require only single- and nearest-neighbor two-qubit gates on two-dimensional arrays of qubits [8], [25]. The planar surface code with code distance d has a $(2d-1) \times (2d-1)$ square grid of qubits of which $d^2 + (d-1)^2$ data qubits are used to encode the logical qubit and $2d(d-1)$ measurement qubits are used to extract the syndromes. In Fig. 1, we show the layout of $d = 3$ planar surface code as an example.

In numerical simulations, the ideal logical state $|0\rangle_L$ followed by single-qubit noise is prepared as the initial state. We assume two types of noise model: code-capacity noise model, where the noise occurs in all data qubits with perfect syndrome measurements, and phenomenological noise model, where the noise occurs in all data qubits and measurement qubits just before the syndrome measurements. The number of rounds of the syndrome measurement in the latter case is d. We also assume that the syndrome measurements are performed perfectly at the final cycle. In both cases, Z-type and X-type errors are uncorrelated, and hence only X-type errors and syndrome measurements are simulated for simplicity. The specific noise channel $\mathcal{N}_{\mathrm{coh}}$ simulated in this work is a mixture of coherent and incoherent noise which is modeled by the over-rotation noise followed by the bit-flip X error as,

$$\mathcal{N}_{\mathrm{coh}} \coloneqq \mathcal{N}_{\mathrm{bit\text{-}flip}} \circ \mathcal{N}_{\mathrm{over\text{-}rot}},$$
$$\mathcal{N}_{\mathrm{over\text{-}rot}} \coloneqq \left[e^{ir\theta X}\right],$$
$$\mathcal{N}_{\mathrm{bit\text{-}flip}} \coloneqq (1-p)[I] + p[X],$$

where $[A]$ is a superoperator defined as $[A]\rho \coloneqq A\rho A^\dagger$, and θ is chosen such that $p = \sin^2 \theta$. We vary the parameters (r, p) and evaluate the performance of the code by using the method described in Sec. 2.
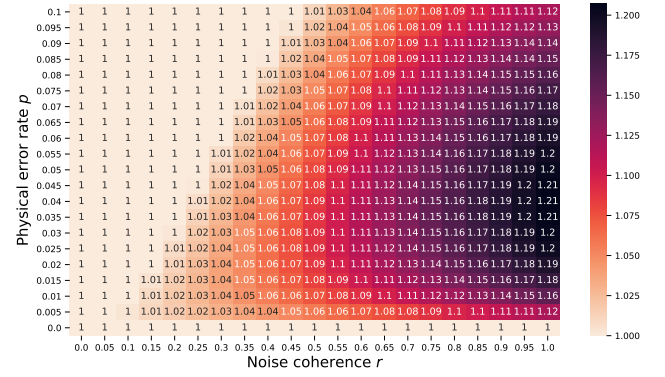
We first examine the sampling cost of our simula-

図 2 Channel robustness of the coherent noise $R_{*\mathrm{coh}}(r, p)$. The horizontal and vertical axis display the noise coherence r and physical error rate p, respectively. Numbers in each cell shows the value of $R_{*\mathrm{coh}}(r, p)$.

tion which is characterized by the channel robustness $R_{*\mathrm{coh}}(r, p)$ of $\mathcal{N}_{\mathrm{coh}}$ [15], [19], [20]. The CSP channels employed to decompose $\mathcal{N}_{\mathrm{coh}}$ are $[I]$, $[X]$, $\left[e^{-i(\pi/4)X}\right]$, and $\left[Xe^{-i(\pi/4)X}\right]$. Figure 2 shows the values of $R_{*\mathrm{coh}}(r, p)$. From Fig. 2, we confirm that the channel robustness increases as the noise coherence becomes larger as expected. Importantly, for a small r with a sufficiently large p, the channel robustness decreases and hits 1.0, where an efficient simulation of coherent errors can be performed. This is because $r\theta$ is small in this region, resulting in the low channel robustness of $\mathcal{N}_{\mathrm{over\text{-}rot}}$. Thus, the bit-flip noise with large p can easily make the channel robustness 1.0. On the other hand, at $p = 0$, the channel robustness of $\mathcal{N}_{\mathrm{over\text{-}rot}}$ is unity even if $r > 0$ since we set $p = \sin^2 \theta$. Therefore certain mixture of incoherent and coherent errors, for example, with $p = 1\%$ (0.1%) and $r = 0.10$ ($r = 0.46$), can be efficiently simulated without any additional overhead, which is in an experimentally important parameter region. This greatly improves the simulation cost over Ref. [16] which is a result of decomposing $\mathcal{N}_{\mathrm{coh}}$ as a whole rather than decomposing $\mathcal{N}_{\mathrm{over\text{-}rot}}$ and $\mathcal{N}_{\mathrm{bit\text{-}flip}}$ individually.

The number of samples needed for accurate results is determined by $R_{*\mathrm{tot}}^2$ via Eq. (5). In the case of the code capacity noise, $\mathcal{N}_{\mathrm{coh}}$ is applied for $d^2 + (d-1)^2$ times, which corresponds to the number of data qubits. Therefore, $R_{*\mathrm{tot}}^2 = (R_{*\mathrm{coh}}(r, p))^{2\left(d^2 + (d-1)^2\right)}$. In the case of the phenomenological noise, $\mathcal{N}_{\mathrm{coh}}$ is applied to each of $d^2 + (d-1)^2$ data qubits for d times and $d(d-1)^2$ measurement qubits for X-type errors for $d-1$ times since we assume perfect measurement in the final round. Overall, $\mathcal{N}_{\mathrm{coh}}$ is applied for $d\left(3d^2 - 4d + 2\right)$ times, which means $R_{*\mathrm{tot}}^2 = (R_{*\mathrm{coh}}(r, p))^{2d\left(3d^2 - 4d + 2\right)}$ in this case. These for-
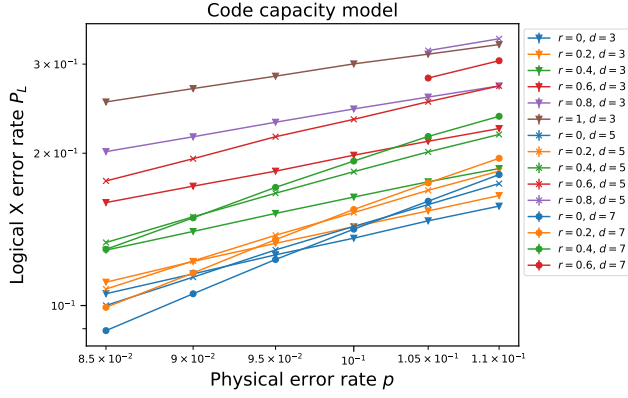
(a)
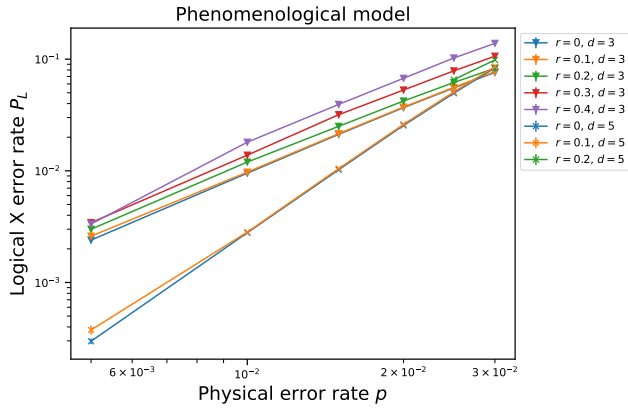
(b)

図 3 Logical X error rate of the planar surface code under the coherent noise as a function of the physical error rate p and noise coherence r in the case of code capacity (a) and phenomenological (b) noise. The horizontal axis shows the physical error rate p, and the vertical axis shows the logical X error rate p_L. The triangles, crosses, and circles stand for $d = 3, 5, 7$ respectively. The color shows the noise coherence.

mulae for $R_{*\mathrm{tot}}^2$ provides us estimates of simulation cost for a given (p, r, d), based on which we choose the parameter range investigated below.

Figure 3 shows the logical error rate p_L as a function of physical error rate p and noise coherence r, where the parameters are chosen such that our workstation with Intel Xeon CPU v4 CPU (E5-2687W), 24 cores, 3.00GHz, can calculate each point within a few days at most. We confirmed that the standard error of each data point is below 10^{-3}. From Fig. 3, the logical error rate increases as the noise coherence grows, which implies that the impact of the coherent noise on the logical error probability is not negligible even for a relatively large code distance. Note that the $d = 5$ code, which requires 81 qubits, is well beyond the reach of naive full state-vector simulation. Furthermore, it is the first analysis of this region
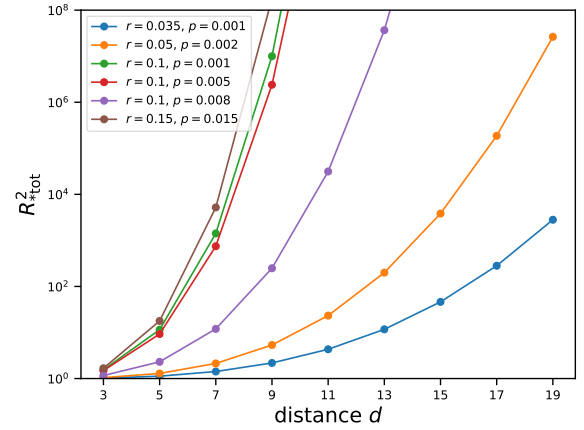

図 4 Scaling of the overhead caused by the quasi-probability sampling, $R_{*\mathrm{tot}}^2$, as a function of the code distance d.

with faulty syndrome measurements to the best of our knowledge.

Finally, let us discuss with which parameters and code distance the proposed method works. Figure 4 shows the dependence of $R_{*\mathrm{tot}}^2$ with respect to d for the phenomenological noise model. Note that for the parameters where $R_{*\mathrm{coh}}(r, p) = 1$ in Fig. 2, we can simulate without any additional overhead as mentioned before. We will be able to simulate large code distances in that region. Outside of that, we expect regions with $R_{*\mathrm{tot}} < 10^3$ are within reach if a high-performance parallel computer of 10^6 CPU cores is available. For example, realistic parameters such as $(p, r, d) = (1.5\%, 0.15\%, 7)$ and $= (0.2\%, 0.05, 13)$ result in $R_{*\mathrm{tot}} < 10^3$. Full state-vector simulation would not work for these numbers of qubits; we need 169 qubits for $d = 7$ and 625 qubits for $d = 13$.

4. Conclusion

We have proposed the sampling-based method to estimate the logical error rate of QEC codes under coherent noise such as an over-rotation error. The simulation protocol is based on the quasi-probability decomposition of noise channels into Clifford operations. It is interesting to note that the QEC process is simulated as usual for sampled CSP channels, and hence the probability distribution for the syndrome measurements is far different from the true one $p(b)$. However, if we sample whether the decoding successes or fails with the quasi-probability method we can estimate the logical error rate. By calculating the channel robustness for the mixture of coherent and incoherent errors, we reduce the simulation costs substantially, which allows us to simulate a practically important parameter

region with a relatively large code distance without any additional overhead or with a reasonable additional overhead. While we have only considered the phenomenological noise model, it is straightforward to extend our method to the circuit-level noise model, where each elementary gate is followed by noise. We leave these problems for future works. We believe that this work helps to analyze the performance of the near-term small-scale QEC in realistic situations.

参考文献

[1] Shor, P. W.: Scheme for Reducing Decoherence in Quantum Computer Memory, *Phys. Rev. A*, Vol. 52, No. 4, pp. R2493–R2496 (online), available from ⟨https://link.aps.org/doi/10.1103/PhysRevA.52.R2493⟩ (1995).

[2] Steane, A.: Multiple-Particle Interference and Quantum Error Correction, *Proc. R. Soc. A*, Vol. 452, No. 1954, p. 19960136 (online), available from ⟨https://royalsocietypublishing.org/doi/abs/10.1098/rspa.1996.0136⟩ (1996).

[3] Kelly, J., Barends, R., Fowler, A. G., Megrant, A., Jeffrey, E., White, T. C., Sank, D., Mutus, J. Y., Campbell, B., Chen, Y., Chen, Z., Chiaro, B., Dunsworth, A., Hoi, I.-C., Neill, C., O'Malley, P. J. J., Quintana, C., Roushan, P., Vainsencher, A., Wenner, J., Cleland, A. N. and Martinis, J. M.: State Preservation by Repetitive Error Detection in a Superconducting Quantum Circuit, *Nature*, Vol. 519, No. 7541, pp. 66–69 (online), available from ⟨https://www.nature.com/articles/nature14270⟩ (2015).

[4] Egan, L., Debroy, D. M., Noel, C., Risinger, A., Zhu, D., Biswas, D., Newman, M., Li, M., Brown, K. R., Cetina, M. and Monroe, C.: Fault-Tolerant Operation of a Quantum Error-Correction Code, *arXiv:2009.11482 [quant-ph]*, (online), available from ⟨http://arxiv.org/abs/2009.11482⟩ (2021).

[5] Chen, Z., Satzinger, K. J., Atalaya, J., Korotkov, A. N., Dunsworth, A., Sank, D., Quintana, C., McEwen, M., Barends, R., Klimov, P. V., Hong, S., Jones, C., Petukhov, A., Kafri, D., Demura, S., Burkett, B., Gidney, C., Fowler, A. G., Putterman, H., Aleiner, I., Arute, F., Arya, K., Babbush, R., Bardin, J. C., Bengtsson, A., Bourassa, A., Broughton, M., Buckley, B. B., Buell, D. A., Bushnell, N., Chiaro, B., Collins, R., Courtney, W., Derk, A. R., Eppens, D., Erickson, C., Farhi, E., Foxen, B., Giustina, M., Gross, J. A., Harrigan, M. P., Harrington, S. D., Hilton, J., Ho, A., Huang, T., Huggins, W. J., Ioffe, L. B., Isakov, S. V., Jeffrey,

E., Jiang, Z., Kechedzhi, K., Kim, S., Kostritsa, F., Landhuis, D., Laptev, P., Lucero, E., Martin, O., Mc-Clean, J. R., McCourt, T., Mi, X., Miao, K. C., Mohseni, M., Mruczkiewicz, W., Mutus, J., Naaman, O., Neeley, M., Neill, C., Newman, M., Niu, M. Y., O'Brien, T. E., Opremcak, A., Ostby, E., Pató, B., Redd, N., Roushan, P., Rubin, N. C., Shvarts, V., Strain, D., Szalay, M., Trevithick, M. D., Villalonga, B., White, T., Yao, Z. J., Yeh, P., Zalcman, A., Neven, H., Boixo, S., Smelyanskiy, V., Chen, Y., Megrant, A. and Kelly, J.: Exponential Suppression of Bit or Phase Flip Errors with Repetitive Error Correction, *arXiv:2102.06132 [quant-ph]*, (online), available from ⟨http://arxiv.org/abs/2102.06132⟩ (2021).

[6] Gottesman, D. E.: Stabilizer Codes and Quantum Error Correction, PhD Thesis, California Institute of Technology (1997).

[7] Aaronson, S. and Gottesman, D.: Improved Simulation of Stabilizer Circuits, *Phys. Rev. A*, Vol. 70, No. 5, p. 052328 (online), available from ⟨https://link.aps.org/doi/10.1103/PhysRevA.70.052328⟩ (2004).

[8] Fowler, A. G., Whiteside, A. C. and Hollenberg, L. C. L.: Towards Practical Classical Processing for the Surface Code, *Phys. Rev. Lett.*, Vol. 108, No. 18, p. 180501 (online), available from ⟨https://link.aps.org/doi/10.1103/PhysRevLett.108.180501⟩ (2012).

[9] Jurcevic, P., Javadi-Abhari, A., Bishop, L. S., Lauer, I., Bogorin, D. F., Brink, M., Capelluto, L., Günlük, O., Itoko, T., Kanazawa, N., Kandala, A., Keefe, G. A., Krsulich, K., Landers, W., Lewandowski, E. P., McClure, D. T., Nannicini, G., Narasgond, A., Nayfeh, H. M., Pritchett, E., Rothwell, M. B., Srinivasan, S., Sundaresan, N., Wang, C., Wei, K. X., Wood, C. J., Yau, J.-B., Zhang, E. J., Dial, O. E., Chow, J. M. and Gambetta, J. M.: Demonstration of Quantum Volume 64 on a Superconducting Quantum Computing System, *Quantum Sci. Technol.*, Vol. 6, No. 2, p. 025020 (online), available from ⟨https://doi.org/10.1088/2058-9565/abe519⟩ (2021).

[10] Sheldon, S., Bishop, L. S., Magesan, E., Filipp, S., Chow, J. M. and Gambetta, J. M.: Characterizing Errors on Qubit Operations via Iterative Randomized Benchmarking, *Phys. Rev. A*, Vol. 93, No. 1, p. 012301 (online), available from ⟨https://link.aps.org/doi/10.1103/PhysRevA.93.012301⟩ (2016).

[11] Tomita, Y. and Svore, K. M.: Low-Distance Surface Codes under Realistic Quantum Noise, *Phys. Rev. A*, Vol. 90, No. 6, p. 062320 (online), available from ⟨https://link.aps.org/doi/10.1103/PhysRevA.90.062320⟩ (2014).

[12] Darmawan, A. S. and Poulin, D.: Tensor-Network Simulations of the Surface Code under Realistic Noise, *Phys. Rev. Lett.*, Vol. 119, No. 4, p. 040502 (online), available from ⟨http://link.aps.org/doi/10.1103/PhysRevLett.119.040502⟩ (2017).

[13] Suzuki, Y., Fujii, K. and Koashi, M.: Efficient Simulation of Quantum Error Correction Under Coherent Error Based on the Nonunitary Free-Fermionic Formalism, *Phys. Rev. Lett.*, Vol. 119, No. 19, p. 190503 (online), available from ⟨https://link.aps.org/doi/10.1103/PhysRevLett.119.190503⟩ (2017).

[14] Bravyi, S., Englbrecht, M., König, R. and Peard, N.: Correcting Coherent Errors with Surface Codes, *npj Quantum Inf.*, Vol. 4, No. 1, pp. 1–6 (online), available from ⟨https://www.nature.com/articles/s41534-018-0106-y⟩ (2018).

[15] Seddon, J. R. and Campbell, E. T.: Quantifying Magic for Multi-Qubit Operations, *Proc. R. Soc. A*, Vol. 475, No. 2227, p. 20190251 (online), available from ⟨https://royalsocietypublishing.org/doi/10.1098/rspa.2019.0251⟩ (2019).

[16] Bennink, R. S., Ferragut, E. M., Humble, T. S., Laska, J. A., Nutaro, J. J., Pleszkoch, M. G. and Pooser, R. C.: Unbiased Simulation of Near-Clifford Quantum Circuits, *Phys. Rev. A*, Vol. 95, No. 6, p. 012301 (online), available from ⟨http://link.aps.org/doi/10.1103/PhysRevA.95.062337⟩ (2017).

[17] Stahlke, D.: Quantum Interference as a Resource for Quantum Speedup, *Phys. Rev. A*, Vol. 90, No. 2, p. 022302 (online), available from ⟨https://link.aps.org/doi/10.1103/PhysRevA.90.022302⟩ (2014).

[18] Pashayan, H., Wallman, J. J. and Bartlett, S. D.: Estimating Outcome Probabilities of Quantum Circuits Using Quasiprobabilities, *Phys. Rev. Lett.*, Vol. 115, No. 7, p. 070501 (online), available from ⟨https://link.aps.org/doi/10.1103/PhysRevLett.115.070501⟩ (2015).

[19] Howard, M. and Campbell, E.: Application of a Resource Theory for Magic States to Fault-Tolerant Quantum Computing, *Phys. Rev. Lett.*, Vol. 118, No. 9, p. 090501 (online), available from ⟨https://link.aps.org/doi/10.1103/PhysRevLett.118.090501⟩ (2017).

[20] Hakkaku, S. and Fujii, K.: Comparative Study of Sampling-Based Simulation Costs of Noisy Quantum Circuits, *Phys. Rev. Applied*, Vol. 15, No. 6, p. 064027 (online), available from ⟨https://link.aps.org/doi/10.1103/PhysRevApplied.15.064027⟩ (2021).

[21] Mitarai, K. and Fujii, K.: Overhead for Simulating a Non-Local Channel with Local Channels by Quasiprobability Sampling, *Quantum*, Vol. 5, p. 388 (online), available from ⟨https://quantum-journal.org/papers/q-2021-01-28-388/⟩ (2021).

[22] Seddon, J. R., Regula, B., Pashayan, H., Ouyang, Y. and Campbell, E. T.: Quantifying Quantum Speedups: Improved Classical Simulation From Tighter Magic Monotones, *PRX Quantum*, Vol. 2, No. 1, p. 010345 (online), available from ⟨https://link.aps.org/doi/10.1103/PRXQuantum.2.010345⟩ (2021).

[23] Hoeffding, W.: Probability Inequalities for Sums of Bounded Random Variables, *J. Am. Stat. Assoc.*, Vol. 58, No. 301, pp. 13–30 (online), available from ⟨https://www.jstor.org/stable/2282952⟩ (1963).

[24] Dennis, E., Kitaev, A., Landahl, A. and Preskill, J.: Topological Quantum Memory, *J. Math. Phys.*, Vol. 43, No. 9, pp. 4452–4505 (online), available from ⟨https://aip.scitation.org/doi/10.1063/1.1499754⟩ (2002).

[25] Kitaev, A.: Fault-Tolerant Quantum Computation by Anyons, *Ann. Phys. (N. Y.)*, Vol. 303, No. 1, pp. 2–30 (online), available from ⟨https://linkinghub.elsevier.com/retrieve/pii/S0003491602000180⟩ (2003).